Validating production of PET radionuclides in solid and liquid targets: Comparing Geant4 predictions with FLUKA and measurements

T. Amin[a], A. Infantino[b], R. Barlow[a], C. Hoehr[c,*]

[a] University of Huddersfield, Huddersfield HD1 3DH, UK
[b] European Organization for Nuclear Research, CH-1211 Geneva 23, Switzerland
[c] TRIUMF, Vancouver BC V6T 2A3, Canada

HIGHLIGHTS

- Geant4 useful tool for simulation of PET isotope production.
- Geant4 and FLUKA results consistent.
- Geant4 using TENDL cross sections with QGSP-AllHP model best compromise.
- Model QGSP-BERT-HP and QGSP-BIC-HP do not produce all isotopes.

ARTICLE INFO

ABSTRACT

The Monte Carlo toolkit Geant4 is used to simulate the production of a number of positron emitting radionuclides: ^{13}N, ^{18}F, ^{44}Sc, ^{52}Mn, ^{55}Co ^{61}Cu, ^{68}Ga, ^{86}Y, ^{89}Zr and ^{94}Tc, which have been produced using a 13 MeV medical cyclotron. The results are compared to previous simulations with the Monte Carlo code FLUKA and experimental measurements. The comparison shows variable degrees of agreement for different isotopes. The mean absolute deviation of Monte Carlo results from experiments was 1.4 ± 1.6 for FLUKA and 0.7 ± 0.5 for Geant4 using TENDL cross sections with QGSP-BIC-AllHP physics. Both agree well within the large error, which is due to the uncertainties present in both experimentally determined and theoretical reaction cross sections. Overall, Geant4 has been confirmed as a tool to simulate radionuclide production at low proton energy.

1. Introduction

Radioisotopes play a crucial role in the diagnosis and treatment of cancer. Numerous isotope-producing nuclear reactors are due to end their operation within a few years. As a result, proton-induced reactions have attracted significant interest from the scientific community after cyclotrons proved to be a feasible alternative to reactor produced radioisotopes (Bénard et al., 2014; Schaffer et al., 2015). Currently cyclotrons can be used to produce radioisotopes for imaging techniques such as positron emission tomography (PET) and single photon emission computed tomography (SPECT). The irradiated target can be in solid, liquid or gaseous form and may be required to satisfy strict design constraints. For example, a target may have material composition restrictions to achieve a desired specific activity, proton energy constraints to avoid unwanted isotope production, or may need to survive several hours of proton irradiation without any thermal issues. As a result, cyclotron targets and materials can be very expensive. Monte Carlo (MC) simulations can be used to assess the expected yield and to optimize target design and materials to maximize yield of the isotope of interest without increasing the production of contaminants (Infantino et al., 2011; Remetti et al., 2011; Sadeghi et al., 2013; Fassbender et al., 2007). The success in using MC for yield assessment depends strongly on the cross section data used for the simulation. Despite a large number of experiments carried out with proton activation, the data available are often inconsistent and at times data from different experiments conflict with each other.

In this work, the MC package Geant4 has been used to simulate the yields of the following PET isotopes: ^{13}N, ^{18}F, ^{44}Sc, ^{52}Mn, ^{55}Co ^{61}Cu, ^{68}Ga, ^{86}Y, ^{89}Zr and ^{94}Tc. The results have been compared to our previous work with the MC package FLUKA and with experiments (Infantino et al., 2016). Different physics models in Geant4 have been tested to find the best approximator of isotopic yield to experiments. Previous results for ^{13}N, ^{18}F, and ^{68}Ga have been published (Amin et al., 2017) and are repeated here for completeness.

---

* Corresponding author.
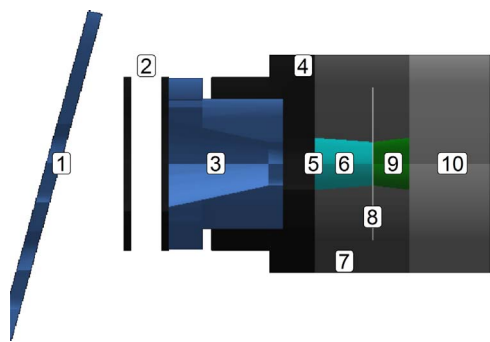 *E-mail address:* choehr@triumf.ca (C. Hoehr).

Fig. 1. Liquid target.

2. Materials and methods

2.1. Experiments

The experimental details have been described and, where appropriate, referenced by Infantino et al. (2016). Some details are repeated here for the convenience of the reader.

The TR13 cyclotron is located at TRIUMF, Vancouver, Canada and used for routine production of medical isotopes. It is self shielded and accelerates negative hydrogen ions to 13 MeV energy with currents of routinely up to 25 μA. Extraction occurs with the use of a carbon foil which strips off the two electrons thus reversing the charge and bending trajectory of the ion in the magnetic field. The cyclotron has two extraction ports with a target selector, which can move the target into the proton beam. Further details of the cyclotron are provided by Laxdal et al. (1994); Buckley et al. (2000).

The selector has four positions, allowing eight different targets to be installed at a time. Two target assemblies were simulated in Geant4. Figs. 1 and 2 illustrate the liquid and solid target assemblies respectively with each component labeled numerically. The proton beam enters the assembly though the baffle (1) and collimator rings (2). The beam is then collimated further with a four quadrant conical collimator (3) contained within an insulator flange (4). Each quadrant of the collimator is capable of measuring beam current separately and the four readings can be used to deduce the position of the proton beam. The beam then enters the target assembly through a 25 μm thick aluminium foil (5), which separates the cyclotron vacuum from the target assembly. Due to the power deposition in the foil, helium cooling (6) is applied to the foil in the helium window (7).

The liquid target (9) is a closed volume of 0.9 ml capacity, with 8 mm depth and 12 mm diameter. The liquid target is separated from the helium cooling (6) by a HAVAR foil (8). HAVAR is a cobalt based metal alloy with high tensile strength. It is composed of 42.5% cobalt, 13.0% nickel, 20.0% chromium, 2.0% molybdenum, 0.2% carbon, 0.04% beryllium, 1.6% manganese, 2.8% tungsten and remainder iron, see Hamilton Precision Metals (2017). The target body (10) is
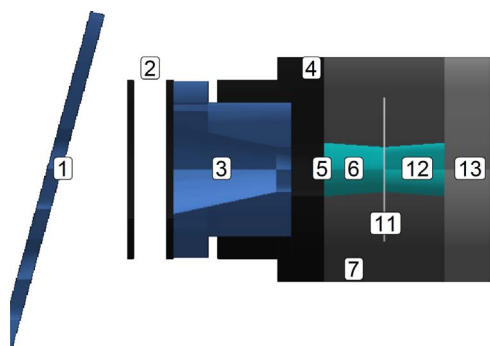

Fig. 2. Solid target.

composed of standard niobium. Target loading and unloading is performed using an automated loading system, see Hoehr et al. (2014).

In the solid target assembly, the foil target (11) is in the place of the HAVAR with helium jets for cooling on both sides (6) and (12). Due to the use of thin foils, the proton beam traverses through the target and is finally stopped by the water cooled aluminium block (13) which acts as the beam dump. The geometries were modelled as accurately as possible by using dimensions from technical drawings.

The nuclear and chemical properties of the liquid and solid target materials are listed in Table 1. After irradiation, isotopic yield measurements were performed using gamma-ray spectrometry analysis or ionization chamber measurements. All measured yields were decay-corrected to the end of bombardment (EOB). When multiple irradiations took place for the same isotope, the yield was normalized to the beam current prior to calculating the average saturation yield. The error in the yield is dominated by the standard deviation of the different irradiations. For more details see Infantino et al. (2016) and references therein.

2.2. Monte Carlo simulations

Geant4 is an all particle Monte Carlo toolkit designed for simulating particle interactions from 100 TeV down to a few eV. Geant4 is implemented in C++ and has great flexibility and expandability and thus is used in various applications such as space research, Large Hadron Collider (LHC) experiments, medical physics or microdosimetry applications (Agostinelli et al., 2003; Allison et al., 2006, 2016).

2.2.1. Saturation yields

In Geant4, the calculation of induced activity relies on the cross section library used for the inelastic nuclear reactions. These cross sections are included in the TENDL1.3 package and can directly calculate the number of isotopes produced. The production rate for each isotope is simulated taking into account primary proton impact, secondary interactions and decay of other isotopes produced in these interactions. Geant4 calculates the isotope production from the primary particle induced production and also the full Bateman solution considering the breeding of radioactive decay products. The number of isotopes at any given time t during the irradiation is given by:

$$N(t) = \frac{nI}{n_p e\lambda}[1 - e^{(-\lambda t)}] \tag{1}$$

where n is the number of isotopes produced per unit mass and unit time (a function of the proton flux, the target density, and the nuclear cross section), I is the proton beam current from the accelerator, n_p is the number of incident protons, e is the proton electric charge, and λ is the decay constant of the isotope, see Bungau et al. (2014). This equation reaches a saturation level for long irradiation, N_{sat}, where $N_{sat} = \frac{nI}{n_p e\lambda}$. Using $A_{sat} = N_{sat}\lambda$, the saturation yield Y_{sat} in $Bq/\mu A$ is given by:

$$Y_{sat} = \frac{A_{sat}}{I} \tag{2}$$

When calculating yield ratios the experimental and MC uncertainties have been added in quadrature.

2.2.2. Target geometry and material definition

The solid and liquid targets have been represented in Geant4 using two geometries as shown in Figs. 1 and 2. Geant4 provides a wide range of simple solid geometries that can be used. More complex geometries such as the conical collimator can be generated by combining existing shapes with Boolean operators such as G4UnionSolid and G4SubtractionSolid.

The target materials have been divided into two categories: liquid target, containing water solution of salts, and solid targets. While it is possible to use the natural isotopic composition of elements from the NIST database, user defined isotopic compositions were used in order to

Table 1
Definitions and properties of target materials.

Production reaction	Half life	mean beta energy	positron yield	Liquid targets	Solution density [g/cm³]	Additional Chemicals	Weight fraction salt	Weight fraction water	Weight fraction solv.
$^{nat}O(p,x)^{13}N$	10 min	492 keV	100%	$H_2^{nat}O$	1.00	H_2O_2	–	0.994	0.006
$^{18}O(p,n)^{18}F$	110 min	20 keV	97%	$H_2^{18}O$ (96% enrich.)	1.00	–	–	0.96	–
$^{nat}Ca(p,x)^{44}Sc$	3.97 h	250 keV	97%	$^{nat}Ca(NO_3)_2 \cdot 4\,H_2O$	1.55	–	0.684	0.316	–
$^{nat}Zn(p,x)^{68}Ga$	68 min	836 keV	88%	$^{nat}Zn(NO_3)_2 \cdot 6\,H_2O$	1.56	Conc. HNO_3	0.743	0.225	0.032
$^{nat}Sr(p,x)^{86}Y$	14.74 h	660 keV	31.9%	$^{nat}Sr(NO_3)_2$	1.43	–	0.636	0.364	–
$^{89}Y(p,x)^{89}Zr$	78 h	395.5 keV	22.7%	$^{89}Y(NO_3)_3 \cdot 6\,H_2O$	1.43	Conc. HNO_3	0.504	0.454	0.042
$^{nat}Mo(p, x)^{94m}Tc$	52 min	2.438 MeV	70.2%	$((NH_4)_6^{nat}Mo_7O_{24}) \cdot 4\,H_2O$	0.995	H_2O_2	0.599	0.361	0.040
				Solid Targets	Density [g/cm³]	Purity	Thickness [mm]	Diameter [mm]	
$^{nat}Cr(p,x)^{52}Mn$	5.6 days	224.6 keV	26.9%	^{nat}Cr	7.180	99.99	0.5	32	
$^{nat}Ni(p,x)^{55}Co$	17.5 h	570 keV	77%	^{nat}Ni	8.902	99.99	0.25	32	
$^{nat}Zn(p,x)^{61}Cu$	3.4 h	1.2 MeV	61%	^{nat}Zn	7.133	99.99	0.1	32	

match material definitions in the FLUKA model in Infantino et al. (2016). For solid and liquid targets, the mass fractions were calculated for each element and used in the definition of materials.

2.2.3. Physics models

Geant4 provides multiple (data-driven, parametrized and theory-driven) physics models, each applicable for different particle interactions at different energy levels. In this study, in order to model proton (and neutron) inelastic hadronic interactions in the relevant energy range, three physics lists were considered: Bertini Intranuclear Cascade High Precision (QGSP-BERT-HP) model, Binary Intranuclear Cascade High Precision (QGSP-BIC-HP) model and Binary Intranuclear Cascade All High Precision (QGSP-BIC-AllHP) model. In Geant4 QGSP-BERT-HP and QGSP-BIC-HP are well established physics list for low energy application but were not developed for predicting radionuclide production. From the three physics lists investigated, QGSP-BIC-AllHP proved to be the best approximator for our investigation. The QGSP-BERT-HP list failed to calculate any yield for ^{13}N and ^{61}Cu. QGSP-BIC-HP did not calculate any ^{13}N yield. Due to these limitations, mainly results from the QGSP-BIC-AllHP physics list are being discussed in this paper.

QGSP-BIC-AllHP is a new data-driven all particle, high precision physics model that uses TALYS-based Evaluated Nuclear Data Library (TENDL). TENDL is based on experimental and calculated results of TALYS nuclear model code to produce a nuclear data library for Alpha, Deuteron, ^{3}He, Proton, Neutron and Triton for energies below 200 MeV. The proton sub-library contains cross sections of about 2800 isotopes. This model has been validated against experimental data (Koning and Rochman, 2012). In this work TENDL 2015 cross sections were used with Geant4 10.1 for energies below 200 MeV.

To describe electromagnetic interactions, electromagnetic options 1, 2 and 3 were tested. Electromagnetic option 1 proved to produce comparable results with the benefit of reduced computation time. The production thresholds were set at 1 mm for all particles inside the target volume.

2.2.4. Proton beam and scoring

In this work, isotopic yields have been normalized to beam current on the target. Since collimated protons do not contribute to yields, but consume simulation time, a idealized pencil beam was used in simulations. The parameters scored in the simulation were secondary nucleons produced due to inelastic protons interactions, N and number of protons incident on the solid or liquid target, n_p. For isotopes in excited states, the yield is presented as the sum of the metastable and ground states. Inside the target volume, 100 μm and 1 μm binning was used for the liquid and solid target respectively. To achieve statistical uncertainties in the yield of less than 1%, for the isotopic yield of interest, numbers of primaries simulated were between $10^9 - 10^{10}$.

2.2.5. External cross sections

As the saturation yield is a function of the nuclear reaction cross section in the energy range between the beam entering the target to the beam exiting the target or being stopped, see Infantino et al. (2016), comparing the area under the cross section in this energy range between experimental and TENDL cross sections is a good measure of the expected yield difference. Experimental Nuclear Reaction Data cross sections were taken from EXFOR (IAEA, 2017). For reactions with multiple available sources, selections were performed taking into account error margins and the number of data points available for the energy range concerned. The source(s) of experimental reaction cross sections for every isotope investigated are listed in Table 2 under the reference column. After selecting appropriate cross sections, a curve was fitted through the cross sections, and the area under the curve was calculated for both the EXFOR and the TENDL cross sections. Comparisons between TENDL and EXFOR cross section areas are shown in Table 2.

2.2.6. FLUKA

FLUKA is a Fortran-based general purpose Monte Carlo code used to investigate particle transport and interaction with matter (Ferrari et al., 2005; Boehlen et al., 2014). It is applicable at energies from low (keV) energy to TeV energy levels such as shielding, target design, calorimetry, hadron therapy, neutrino physics, cosmic rays, etc. FLUKA is jointly developed by the European Organization for Nuclear Research (CERN) and the Italian Institute for Nuclear Physics (INFN). The FLUKA MC package version 2011.2b.6 was used for the isotope production at the medical cyclotron. Isotope production in FLUKA is handled inside the software package. Materials were defined by the user to match with experimental details. For more details, see Infantino et al. (2016).

3. Results

3.1. Experimental reference data

Experimental yields including the reference source, and Monte Carlo values used for comparison are listed in Table 2. For each isotope, the saturation yield Y_{exp} and the number of irradiations conducted are reported. The produced activity in each irradiation is normalized to the beam current before calculating the average saturation yield of the given isotope. The yield has been decay-corrected to EOB and normalized for a beam current of 1 μA incident on the target for a 1 h irradiation.

3.2. Direct assessment from Geant4

The isotopic yields calculated in Geant4 are compared with measurements in Table 2. Y_F refers to yield from FLUKA, Y_G refers to Geant4

Table 2
Comparison between experimental (Y_{exp}) to Geant4 (Y_G) and FLUKA (Y_F) saturation yields and TENDL (X_T) with EXFOR (X_E) cross sections.

Isotope	Number of measurements	Y_{exp} [MBq/µA]	Y_F/Y_{exp}	Y_G/Y_{exp}	X_T/X_E	Ref.
^{13}N	12	259 ± 3 Infantino et al. (2016)	5.92 ± 0.01	2.73 ± 0.01	2.34	IAEA-NDS (2015a)
^{18}F	9	4920 ± 60 Infantino et al. (2016)	1.66 ± 0.01	0.53 ± 0.01	0.94	IAEA-NDS (2015b)
^{44}Sc	3	4.9 ± 0.3 Hoehr et al. (2014)	2.35 ± 0.06	2.1 ± 0.1	1.0	Levkovsky (1991) de Waal et al. (1971)
^{52}Mn	5	900 ± 100 Topping et al. (2013)	4.62 ± 0.11	1.1 ± 0.1	0.93	Tanaka and Furukawa (1959)
^{55}Co	4	180 ± 20 Ferreira et al. (2007)	0.3 ± 0.1	0.7 ± 0.1	0.88	Kaufman (1960)
^{61}Cu	3	130 ± 20 Infantino et al. (2016)	3.13 ± 0.15	0.6 ± 0.2	0.55	Levkovsky (1991)
^{68}Ga	3	138 ± 2 Infantino et al. (2016)	1.03 ± 0.02	0.84 ± 0.02	0.75	Levkovsky et al. (1990b) Johnson et al. (1964) Vinogradov et al. (1993) Zhuravlev et al. (1995)
^{86}Y	3	40 ± 50 Infantino et al. (2016)	0.9 ± 1.30	2.5 ± 1	1.0	IAEA-NDS (2015c)
^{89}Zr	6	346 ± 2 Infantino et al. (2016)	0.87 ± 0.01	0.69 ± 0.01	1.22	Levkovsky et al. (1990a) Mustafa et al. (1988) Wenrong and Cheng (1982) Michel et al. (1997) Omara et al. (2009) Khandaker et al. (2012)
^{94}Tc	3	49 ± 6 Hoehr et al. (2012)	1.5 ± 0.1	1.7 ± 0.1	1.16	Levkovsky (1991) Zhuravlev et al. (1994)

yields using TENDL libraries. Table 2 compares the simulated and experimental yields. The table also lists cross section ratios obtained from Fig Fig 3, where the TENDL and EXFOR cross sections (X_T, X_E) have been expressed as ratios of each other. This has been referred to as cross section ratio later in the paper. The cross section ratio can be used to get an approximation of the theoretical yields that can be expected when using the TENDL library. In Fig. 3 only the most probable nuclear reaction cross section was taken into account. However, in MC code incident protons and all secondaries are taken into account. For the reaction ^{nat}Sr(p,x)^{86}Y, the cross section for only ^{86}Sr(p,n)^{86}Y reaction was taken into account as it was the majority contributor to ^{86}Y yield. Contributions from other reactions are assumed to be insignificant to the overall yield and hence not taken into account.

During experiments or routine isotope production, there are losses in the transfer system and in vials prior to measurement for liquid targets and dissolved solid targets respectively. Also MC codes do not take into account complex thermal and fluid dynamics of the liquid target. Thus a factor of 2 seems to be an acceptable limit for the ratio of saturation yield. The comparison between Geant4 and experiment for the isotopes ^{18}F, ^{44}Sc, ^{52}Mn, ^{55}Co, ^{61}Cu, ^{68}Ga, ^{89}Zr, and ^{94}Tc fulfills this criteria. Only for ^{13}N and ^{86}Y is the ratio between Geant4 and experiment larger than 2, and none is smaller than 0.5.

3.2.1. ^{18}F, ^{52}Mn, ^{55}Co, ^{61}Cu, ^{68}Ga, ^{89}Zr, and ^{94}Tc

Overall in this section, Geant4 is less than a factor of two away from the experimental yield. It is also closer to the experimental yield than FLUKA for five isotopes (^{18}F, ^{52}Mn, ^{55}Co, ^{61}Cu, ^{68}Ga), while FLUKA is closer for three isotopes (^{68}Ga, ^{89}Zr, ^{94}Tc). In general the comparison of the EXFOR cross sections with the TENDL cross sections used in Geant4 are within 25% except for ^{61}Cu (0.55).

While the yield of ^{18}F is under-calculated by a factor of 0.53 using Geant4, FLUKA over-estimates it by a factor of 1.66. The database takes into account multiple sources to provide a single unified table of cross sections that has been used. The ^{18}O(p,n)^{18}F reaction has multiple resonances between 2 and 10 MeV with each experiment reporting slightly different peaks. This does not take into account the efficiency of the liquid target system.

For ^{52}Mn, ^{55}Co and ^{61}Cu Geant4 performed better than FLUKA with ratios of 1.1, 0.7 and 0.6 against FLUKA's 4.62, 0.3 and 3.13 respectively. For these solid targets FLUKA appears to be less reliable than Geant4, with all yield ratios outside acceptable limits. For these three isotopes, the yield ratios of Geant4 to experimental values correlate very well to the cross section ratios between TENDL and EXFOR. For ^{52}Mn the yield ratio is 1.1 while the cross section ratio is 0.93, for ^{55}Co yield and cross section ratios are 0.7 and 0.88 respectively.

^{61}Cu has a yield ratio and a cross section ratio of 0.6 and 0.55 respectively. The excellent level of agreement between the yield ratio and cross section ratio indicates that while the Geant4 yield might be different from experiments, it is a consequence of mismatching TENDL and EXFOR cross sections.

For ^{68}Ga FLUKA performed better with a ratio of 1.03 against Geant4's 0.84. The cross section of the ^{68}Zn(p,n)^{68}Ga reaction currently has significant discrepancies, hence multiple sources were taken and a spline fit was used to make comparisons. The TENDL library underestimates yields over the concerned energy range compared to fitted EXFOR with a ratio of 0.75. Geant4 over-calculates the yield of ^{86}Y by a factor of 2.5 whereas the FLUKA yield ratio was 0.9.

The yield for ^{89}Zr was calculated more accurately using FLUKA than Geant4, the respective yield ratios are 0.87 and 0.69 respectively. Both MC codes under-estimate the yield, with Geant4's performance disagreeing with theoretical expectations. The TENDL cross section is higher than most EXFOR tabulated cross sections. This indicates that Geant4 should calculate a yield higher than experiments, however, the yield from both MC codes is lower than that of experiments. At this moment no explanation has been found why the MC results challenge the cross sections available.

Due to Geant4 and FLUKA's inability to calculate metastable isotopes, ^{94m}Tc is presented as the sum of metastable and ground state. For this isotope, Geant4 calculates the yield with a factor of 1.7 whereas FLUKA ratio is 1.53 and the cross section ratio is 1.16. Both MC are able to calculate accurately ^{94}Tc yield, with FLUKA performing slightly better.
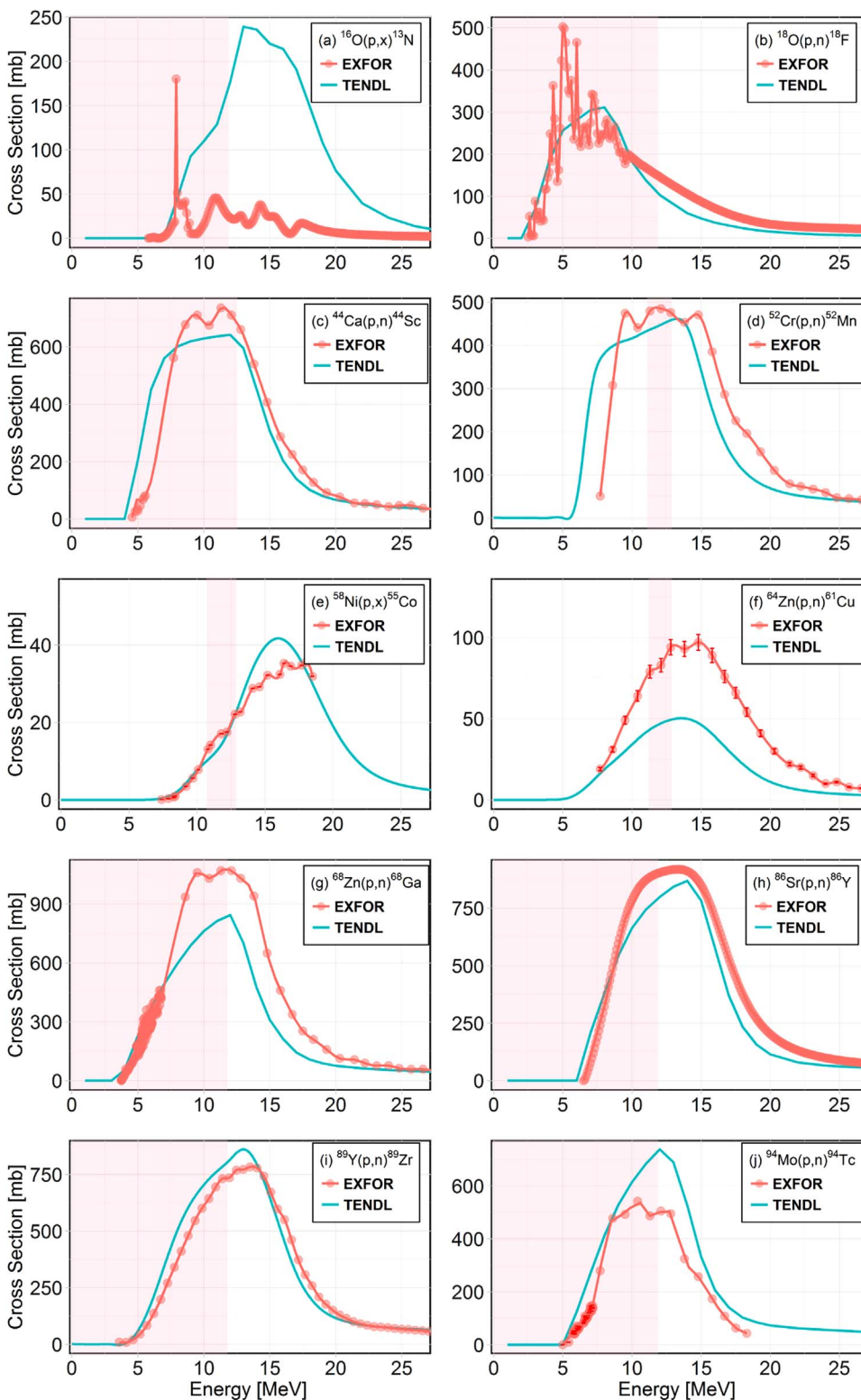
Fig. 3. Comparison of EXFOR and TENDL reaction cross sections for investigated isotopes. The proton energies inside the target are indicated by the shaded regions.

3.2.2. ^{13}N, ^{44}Sc, and ^{86}Y

For these isotopes the deviation from the experiment is larger than a factor of two. For ^{13}N and ^{44}Sc the deviation in the Geant4 simulation is smaller than for FLUKA, while only for ^{86}Y is the deviation for Geant4 larger than for FLUKA. The EXFOR cross section area is the same as the TENDL cross section area, except for ^{13}N which has a very large ratio of 2.34.

^{13}N yield was overestimated by a factor of 2.72 compared to a factor of 5.9 from FLUKA. The yield between Geant4 and experiments of ^{13}N results are not comparable at TR13 energy levels as TENDL does not account for the resonance at 7.9 MeV for the $^{nat}O(p,x)^{13}N$ reaction. For energies above 8.5 MeV, TENDL cross section vastly over-estimate the yield and has large disagreements with EXFOR. This is illustrated by Fig. 3a. This phenomenon was also observed when ^{13}N was created inside a PMMA target under proton therapy conditions in Amin et al. (2017).

For ^{44}Sc FLUKA performed worse with a ratio of 2.35 against Geant4's 2.1. When comparing with experimental cross sections, the ratio for ^{44}Sc is 1.05. While the agreement between ratios is acceptable, EXFOR lacks sufficient good quality cross sections for the reaction of interest at these low energy levels. The contribution of $^{44\,m}$Sc to the total production of ^{44}Sc in MC calculations is negligible for TR13 energy ranges.

Geant4 overestimates the yield of ^{86}Y by a factor of 2.5 whereas the FLUKA yield ratio is a very good 0.9. The yield of ^{86}Y has been represented here as the sum of metastable and ground states of ^{86}Y. As a result, a minor overestimation from Geant4 is expected when comparing simulated yields with experimental yields. The fitted tabulated cross sections for ^{86}Sr(p,x)^{86}Y reaction were provided by the IAEA. The fit was performed using data from Roesch et al. (1993) and Levkovsky et al. (1990a), where the former had significant error bars contributing to a slightly inaccurate smoothing of the fit. Compared to EXFOR, the TENDL data had a marginally larger overall yield in the energy ranges relevant to this work. Despite the discrepancy between the MC codes, the ratio of Geant4 to experimental yields agrees well with the ratio of cross sections for ^{86}Y, as shown is Table 2.

4. Conclusions

A Geant4 simulation to model the liquid and solid target assembly for the TR13 medical cyclotron at TRIUMF has been developed. The agreement between Monte Carlo simulation and experimental yield measurements varies depending on the isotope considered. The physics list QGSP-BIC-AllHP in Geant4 was investigated in this study, a new list recently released with version 10.1. Its performance depends almost entirely on the accuracy of the TENDL cross sections utilized by the user. In our work, TENDL has proven to provide accurate cross sections for certain reactions, whereas for example the ^{16}O(p,x)^{13}N cross section currently is incorrect. For certain isotopes such as ^{68}Ga, ^{86}Y, ^{89}Zr and ^{94}Tc FLUKA was better able to calculate yield. For ^{13}N, ^{18}F, ^{44}Sc, ^{52}Mn, ^{55}Co and ^{61}Cu Geant4 performed better, despite the MC models not accounting for thermal effects or density changes in the liquid target or loss in the transfer system. Overall, in our situation using Geant4 10.1 with the physics list QGSP-BIC-AllHP the mean absolute deviation for all targets is 0.7 ± 0.5 compared to 1.4 ± 1.6 for FLUKA. In addition, QGSP-BERT-HP and QGSP-BIC-HP in Geant4 were also investigated. The QGSP-BERT-HP list managed to produce a slightly lower mean absolute deviation of 0.6 ± 0.4, but failed to calculate any yield for ^{13}N and ^{61}Cu. QGSP-BIC-HP had a mean absolute deviation of 1.1 ± 1.2, failing to calculate any ^{13}N yield. Due to these limitations, neither were further considered. For some isotopes differences are still large. A wider range of isotopes needs to be examined for a better assessment.

Acknowledgements

References

Agostinelli, S., Allison, J., Amako, K., et al., 2003. Geant4–a simulation toolkit. Nucl. Instrum. Methods Phys. Res. Sect. A: Accel. Spectrometers Detect. Assoc. Equip. 506, 250–303.

Allison, J., Amako, K., Apostolakis, J., et al., 2006. Geant4 developments and applications. IEEE Trans. Nucl. Sci. 53, 270–278.

Allison, J., Amako, K., Apostolakis, J., et al., 2016. Recent developments in geant4. Nucl. Instrum. Methods Phys. Res. Sect. A: Accel. Spectrometers, Detect. Assoc. Equip. 835, 186–225.

Amin, T., Infantino, A., Lindsay, C., Barlow, R., Hoehr, C., 2017. Modelling PET radionuclide production in tissue and external targets using Geant4. IOP Conf. Ser.: J. Phys. 874, 012109.

Bénard, F., Buckley, K.R., Ruth, T.J., Zeisler, S.K., Klug, J., Hanemaayer, V., Vuckovic, M., Hou, X., Celler, A., Appiah, J.P., Valliant, J., Kovacs, M.S., Schaffer, P., 2014. Implementation of multi-curie production of $^{99\,m}$Tc by conventional medical cyclotrons. J. Nucl. Med. 55, 1017–1022.

Boehlen, T., Cerutti, F., Chin, M., Fassò, A., Ferrari, A., Ortega, P., Mairani, A., Sala, P., Smirnov, G., Vlachoudis, V., 2014. The FLUKA code: developments and challenges for high energy and medical applications. Nucl. Data Sheets 120, 211–214.

Buckley, K., Huser, J., Jivan, S., Chun, K., Ruth, T., 2000. ^{11}C-methane production in small volume, high pressure gas targets. Radiochim. Acta 88, 201–205.

Bungau, C., Bungau, A., Cywinski, R., Barlow, R., Edgecock, T.R., Carlsson, P., Danared, H., Mezei, F., Holm, A.I.S., Møller, S.P., Thomsen, H.D., 2014. Induced activation in accelerator components. Phys. Rev. Accel. Beams 17, 084701.

de Waal, T.J., Peisach, M., Pretorius, R., 1971. Activation cross sections for proton-induced reactions on calcium isotopes up to 5.6 MeV. J. Inorg. Nucl. Chem. 33, 2783.

Fassbender, M., Arzumanov, A., Jamriska, D., Lyssukhin, S., Trellue, H., Waters, L., 2007. Proton beam simulation with MCNPX: gallium metal activation estimates below 30 MeV relevant to the bulk production of ^{68}Ge and ^{65}Zn. Nucl. Instrum. Methods Phys. Res. Sect. B: Beam Interact. Mater. At. 261, 742–746.

Ferrari A., Sala P.R., Fasso A., Ranft J., 2005. FLUKA: A multi-particle transport code (Program version 2005). CERN-2005-010, SLAC-R-773, INFN-TC-05-11.

Ferreira, C.L., Lapi, S., Steele, J., Green, D.E., Ruth, T.J., Adam, M.J., Orvig, C., 2007. ^{55}Cobalt complexes with pendant carbohydrates as potential PET imaging agents. Appl. Radiat. Isot. 65, 1303–1308.

Hamilton Precision Metals,. Technical Data Sheet. 〈http://www.hpmetals.com/download/Havar.pdf〉; 2017.

Hoehr, C., Morley, T., Buckley, K., Trinczek, M., Hanemaayer, V., Schaffer, P., Ruth, T., Bénard, F., 2012. Radiometals from liquid targets: $^{94\,m}$Tc production using a standard water target on a 13 MeV cyclotron. Appl. Radiat. Isot. 70, 2308–2312.

Hoehr, C., Oehlke, E., Bénard, F., Lee, C.J., Hou, X., Badesso, B., Ferguson, S., Miao, Q., Yang, H., Buckley, K., Hanemaayer, V., Zeisler, S., Ruth, T., Celler, A., Schaffer, P., 2014. $^{44\,g}$Sc production using a water target on a 13 MeV cyclotron. Nucl. Med. Biol. 41, 401–406.

IAEA, 2017. Positron Emitters. 〈https://www-nds.iaea.org/medical/positron_emitters.html〉.

IAEA-NDS, 2015a. Recommended cross sections for ^{16}O(p,a)^{13}N reaction. 〈https://www-nds.iaea.org/medical/o6p13n0.html〉.

IAEA-NDS, 2015b. Recommended cross sections for ^{18}O(p,n)^{18}F reaction. 〈https://www-nds.iaea.org/medical/o8p18f0.html〉.

IAEA-NDS, 2015c. Recommended cross sections for ^{86}Sr(p,n)^{86}Y reaction. 〈https://www-nds.iaea.org/radionuclides/sr6p86y0.html〉.

Infantino, A., Cicoria, G., Pancaldi, D., Ciarmatori, A., Boschi, S., Fanti, S., Marengo, M., Mostacci, D., 2011. Prediction of ^{89}Zr production using the Monte Carlo code FLUKA. Appl. Radiat. Isot. 69, 1134–1137.

Infantino, A., Oehlke, E., Mostacci, D., Schaffer, P., Trinczek, M., Hoehr, C., 2016. Assessment of the production of medical isotopes using the Monte Carlo code FLUKA: simulations against experimental measurements. Nucl. Instrum. Methods Phys. Res. Sect. B: Beam Interact. Mater. At. 366, 117–123.

Johnson, C.H., Trail, C.C., Galonsky, A., 1964. Thresholds for (p,n) Reactions on 26 Intermediate-Weight Nuclei. Phys. Rev. B 136, B1719.

Kaufman, S., 1960. Reactions of protons with ^{58}Ni and ^{60}Ni. Phys. Rev. A 117, 1532–1538.

Khandaker, M.U., Kim, K., Lee, M.W., Kim, K.S., Kim, G., Otuka, N., 2012. Investigations of ^{89}Y(p,x)$^{86,88,89\,g}$Zr, $^{86\,m+g,87\,g,87\,m,88g Y,85\,g}$Sr and $^{84\,g}$Rb nuclear processes up to 42 MeV. Nucl. Instrum. Methods Phys. Res. Sect. B: Beam Interact. Mater. At. 271, 72–81.

Koning, A., Rochman, D., 2012. Modern nuclear data evaluation with the talys code system. Nucl. Data Sheets 113, 2841–2934.

Laxdal R.E., Altman A., Kuo T., 1994. Beam measurements on a small commercial cyclotron. In: Proceedings of the EPAC 94. pp. 1–3.

Levkovsky V., 1991. Cross sections of medium mass nuclide activation (A = 40–100) by medium energy protons and alpha-particles (E = 10–50 MeV). Inter-Vesi.

Levkovsky, V.N., Reutov, V.F., Botvin, K.V., 1990a. Formation of helium in molybdenum, zirconium, niobium, nickel, iron, and chromium under irradiation with 8–30 MeV protons. Sov. J. At. Energy 69, 180.

Levkovsky, V.N., Reutov, V.F., Botvin, K.V., 1990b. Formation of hydrogen in zirconium, niobium, and molybdenum during irradiation with alpha particles in the energy interval from 10 to 46 MeV. Sov. J. At. Energy 69, 99.

Michel, R., Bodemann, R., Busemann, H., Daunke, R., Gloris, M., Lange, H.J., Klug, B., Krins, A., Leya, I., Lupke, M., Neumann, S., Reinhardt, H., Schnatz-Buttgen, M., Herpers, U., Schiekel, T., Sudbrock, F., Holmqvist, B., Conde, H., Malmborg, P., Suter, M., Dittrich-Hannen, B., Kubik, P.W., Synal, H.A., Filges, D., 1997. Cross sections for the production of residual nuclides by low- and medium-energy protons from the target elements C, N, O, Mg, Al, Si, Ca, Ti, V, Mn, Fe, Co, Ni, Cu, Sr, Y, Zr, Nb, Ba and Au. Nucl. Instrum. Methods Phys. Res. B129, 153.

Mustafa, M.G., West, H.I., O'Brien, H., Lanier, R.G., Benhamou, M., Tamura, T., 1988. Measurements and a direct reaction plus Hauser-Feshbach analysis of ^{89}Y(p,n)^{89}Zr, ^{89}Y(p,2n)^{88}, and ^{89}Y(p,pn)^{88}Y reactions up to 40 MeV. Phys. Rev. C 38, 1624–1637.

Omara, H.M., Hassan, K.F., Kandil, S.A., Hegazy, F.E., Saleh, Z.A., 2009. Proton induced reactions on ^{89}Y with particular reference to the production of the medically interesting radionuclide ^{89}Zr. Radiochim. Acta 97, 467.

Remetti, R., Burgio, N.T., Maciocco, L., Arcese, M., Filannino, M.A., 2011. Monte Carlo simulation and radiometric characterization of proton irradiated [^{18}O]H$_2$O for the treatment of the waste streams originated from [^{18}F]FDG synthesis process. Appl. Radiat. Isot. 69, 1046–1051.

Roesch, F., Qaim, S.M., Stocklin, G., 1993. Nuclear data relevant to the production of the positron emitting radioisotope ^{86}Y via the ^{86}Sr(p,n) and (nat)Rb(3He,xn) processes. Radiochim. Acta 61, 1–8.

Sadeghi, M., Jokar, N., Kakavand, T., Fard, H.G., Tenreiro, C., 2013. Prediction of ^{67}Ga production using the Monte Carlo code MCNPX. Appl. Radiat. Isot. 77, 14–17.

Schaffer, P., Bénard, F., Bernstein, A., Buckley, K., Celler, A., Cockburn, N., Corsaut, J.,

Dodd, M., Economou, C., Eriksson, T., Frontera, M., Hanemaayer, V., Hook, B., Klug, J., Kovacs, M., Prato, F., McDiarmid, S., Ruth, T., Shanks, C., Valliant, J., Zeisler, S., Zetterberg, U., Zavodszky, P., 2015. Direct production of $^{99\,m}$Tc via ^{100}Mo(p,2n) on small medical cyclotrons. Phys. Procedia 66, 383–395.

Tanaka, S., Furukawa, M., 1959. Excitation functions for (p,n) reactions with titanium, vanadium, chromium, iron and nickel up to Ep = 14 MeV. J. Phys. Soc. Jpn. 14, 1269–1275.

Topping, G.J., Schaffer, P., Hoehr, C., Ruth, T.J., Sossi, V., 2013. Manganese-52 positron emission tomography tracer characterization and initial results in phantoms and in vivo. Med. Phys. 40, 042502.

Vinogradov, V.M., Zhuravlev, Y.Y., Zarubin, P.P., Kolozhvari, A.A., Sergeev, V.O.,

Sitnikova, I.V., 1993. Excitation functions of (pn) reaction on zinc isotopes in the range of E(p) from 4.9 to 5.9 MeV. Bull. Russ. Acad. Sci.: Phys. 57, 906.

Wenrong, Z., Cheng, G., 1982. Measurement of isomer ratio for ^{133}Cs(n, γ)$^{134\,m,134\,g}$Cs reaction. Chin. J. Nucl. Phys. 4, 54.

Zhuravlev, Y.Y., Zarubin, P.P., Kolozhvari, A.A., 1994. Excitation functions for (pn) reaction on nuclei of Mo isotope in E(p) interval from threshold to 7.2 MeV. Bull. Russ. Acad. Sci.: Phys. 58, 798.

Zhuravlev, Y.Y., Zarubin, P.P., Zeits, Y.V., Kolozhvari, A.A., Shelgunov, I.V., 1995. Excitation functions of (pn) reaction on nuclei of Zn isotopes at E(p) = 5.7–6.8 MeV. Bull. Russ. Acad. Sci.: Phys. 59, 102.